Adsorption of carbon dioxide on hydrotalcite-like compounds of different compositions

Aschenbrenner, O; McGuire, P; Al-Samaq, S; Wang, Jiawei; Supasitmongkol, S; Al-Duri, Bushra; Styring, P; Wood, Joseph

DOI:
10.1016/j.cherd.2010.09.019

Document Version
Early version, also known as pre-print

Citation for published version (Harvard):
Aschenbrenner, O, McGuire, P, Al-Samaq, S, Wang, J, Supasitmongkol, S, Al-Duri, B, Styring, P & Wood, J 2011, 'Adsorption of carbon dioxide on hydrotalcite-like compounds of different compositions', *Chemical Engineering Research and Design*, vol. 89, no. 9, pp. 1711-1721. https://doi.org/10.1016/j.cherd.2010.09.019

Adsorption of carbon dioxide on hydrotalcite-like compounds of different compositions

Ortrud Aschenbrenner[a], Paul McGuire[b], Suzanne Alsamaq[b], Jiawei Wang[b], Somsak Supasitmongkol[a], Bushra Al-Duri[b], Peter Styring[a] and Joseph Wood[*b]

[a]Department of Chemical & Process Engineering, The University of Sheffield, Sir Robert Hadfield Building, Sheffield, UK, S1 3JD.

[b]School of Chemical Engineering, The University of Birmingham, Edgbaston, Birmingham, UK, B15 2TT.

Abstract

The adsorption of carbon dioxide on hydrotalcite-like compounds was investigated. Two different powdered hydrotalcites were used containing the cations nickel and iron. The powdered materials were screened for carbon dioxide adsorption using a thermogravimetric method and it was found that NiMgAl (Sample 1) hydrotalcite has the largest capacity for CO_2, adsorbing 1.58 mmol g^{-1} at 20 °C, and highest rate of adsorption of up to 0.17 mmol g^{-1} min^{-1}. This represented an increase of 53 % in adsorption capacity, compared with NiMgAlFe (Sample 2). In order to improve the rheological behaviour of hydrotalcite paste for extrusion, hydrotalcite powders were combined with boehmite alumina (70:30 and 50:50 ratios of hydrotalcite: boehmite) before extrusion into pellets suitable for use in a fixed bed adsorber. These pellets were then re-crushed and further tested by thermogravimetric methods. The effects of temperature, composition and pre-treatment of the hydrotalcites on the adsorption of carbon dioxide and nitrogen are reported. At 20 °C, the amount of carbon dioxide adsorbed was between 2.0-2.5 mmol g^{-1} for all the hydrotalcite/alumina samples in this study, although this decayed rapidly with increasing temperature. The results are compared

with silica gel as a common sorbent reference, and with literature values. Hydrotalcite/alumina samples have thermal stability and a high adsorption capacity for carbon dioxide over a wide range of temperatures. The composition of the hydrotalcite/alumina pellets investigated in this study has less effect upon the adsorption behaviour compared with the non-calcined hydrotalcite powder, thus allowing a wide choice of pellet compositions to be used.

Keywords: Adsorption, carbon dioxide, hydrotalcite, mixed oxide, carbon capture, thermogravimetric.

1. Introduction

In recent years, the need for reduction of carbon dioxide (CO_2) emissions to prevent the anthropogenic contribution to climate change has become increasingly important (IPCC, 2007). One of the possible ways to achieve this is the capture of carbon dioxide from flue gas in industrial combustion processes and power plants. Various solid materials readily adsorb carbon dioxide. For example, calcium oxide or lithium oxide (Roesch et al., 2005; Mosqueda et al., 2006), silica gel (Wang and Levan, 2009; Huang et al., 2003), zeolites (Majchrzak-Kuceba and Nowak, 2005), activated carbon (Radosz et al., 2008) and hydrotalcites (Hutson and Attwood, 2008; Oliviera et al., 2008; Soares et al., 2005).

Hydrotalcites (Htlc) are a family of clay minerals consisting of a double-layered hydroxide structure, with the general formula $[M^{II}_{x}M^{III}_{(1-x)}(OH)_2][CO_3]_{(1-x)/2}\cdot nH_2O]$ (Cavani et al., 1991). They have a Brucite-like structure, whereby an M^{II} or M^{III} species is substituted almost isomorphously into the edge-sharing $M(OH)_6$ octahedra in place of Mg^{II} to form sheets which have a net positive charge. The cationic sheets stack up on each other yielding a layered structure, with anions in the intercalating layers to balance the charge. Much previous work has concentrated on substituting various metals into the cationic layer (such as Ni^{2+}, (Bhattacharyya et al., 1998; Olafsen et al., 2005; Perez-Lopez et al., 2006; Takehira et al., 2003; Tsyganok et al., 2003) Cu^{2+}, Co^{2+}, Fe^{2+} (Unnikrishnan and Narayanan,

1999; Carja et al., 2001) Cr^{3+} (Kloprogge et al., 2005), Fe^{3+} (Ohisihi et al., 2005) and Mn^{3+} (Barriga et al., 1996), whilst other work has concentrated on substituting various anions into the interstitial layer (Bhattachryya and Hall, 1992; Tamura et al., 2004). Hydrotalcites adsorb carbon dioxide over a wide range of temperatures and can be used in pre-combustion (Walspurger et al., 2008) or post combustion capture (Soares et al., 2005) of carbon dioxide.

The composition (Hutson and Attwood, 2008) and preparation conditions (Kloprogge et al., 2005; Costantino et al., 1998) have been shown to influence the properties of hydrotalcites, such as surface area, and thus the amount of carbon dioxide they can adsorb. For example, addition of potassium as a promoter was found to increase the adsorption of carbon dioxide (Oliveira et al., 2008; Walspurger et al., 2008). The cation substituted into the Brucite layer has been shown to have a strong effect on physicochemical properties, such as surface area, pore structure and reducibility (Chmielarz et al., 2002). The anion also influences the structure of the finished hydrotalcite, particularly influencing the crystallinity and layer spacing (Tsyganok et al., 2003; Bhattacharyya and Hall, 1992; Carpani et al., 2004).

The main requirements for sorbents in carbon dioxide capture from flue gas are high capacity for carbon dioxide, high selectivity over nitrogen, low regeneration energy and high stability during subsequent sorption-desorption cycles. Various experimental data have been published on the adsorption of carbon dioxide on hydrotalcites. However, most of the adsorption studies in the literature were performed with hydrotalcites promoted with potassium or purely containing magnesium and aluminium cations. Few studies can be found about hydrotalcites with different compositions. Of those studies that have been published, Yong and Rodrigues (2002) reviewed progress on adsorption of carbon dioxide upon hydrotalcite like compounds. They found that the type of anion, cation and heat treatment influenced the adsorption capacity of carbon dioxide. Higher heat treatment, an optimal aluminium content and anions containing $CO_3^{2-}/Fe(CN)_6^{4-}$ gave the best adsorption capacities. The optimum alumina content was a trade off between increased density of layer charge with increasing alumina, against decrease in the layer spacing as

alumina content increased. Anions leading to increased void space in the interlayer were found to lead to uptake of more carbon dioxide gas. Wang et al. (2008) studied the high temperature adsorption of carbon dioxide on mixed oxides derived from hydrotalcite like compounds. It was found that, for example, CaCoAlO captures 1.39 mmol g^{-1} of CO_2 from a gas mixture (8 % CO_2 in N_2). Lwin and Abdullah (2009) studied the effect of Cu/Al ratio on the carbon dioxide capture characteristics of mixed oxides derived from hydrotalcites and found that for Cu/Al=1.0 approximately 30 mg g^{-1} (0.68 mmol g^{-1}) carbon dioxide was adsorbed at a temperature of 25 °C. Choi et al. (2009) reviewed the use of hydrotalcites, amongst other materials, for carbon dioxide capture and found that adsorption capacities at elevated temperatures ranged from 0.17 – 0.9 mmol g^{-1} at temperatures of 473 – 773 K. With renewed interest in carbon dioxide capture from stationary sources to comply with reductions in carbon capture emissions, new generations of adsorbents with increased carbon dioxide capture capacity are sought. Therefore there is new scope to further investigate and optimise the formulation of adsorbents such as hydrotalcites to understand what factors control their adsorption capacity and to increase it. In this study we present experimental results for the adsorption of carbon dioxide on hydrotalcites containing NiMgAl and iron (Fe) in different compositions. The effects of temperature and composition on stability, adsorption capacity and selectivity are discussed. The results are compared with silica gel as a cheap and available common sorbent.

2. Experimental

2.1. Preparation of the samples

2.1.1. Hydrotalcite preparation

NiMgAl hydrotalcites were prepared by the co-precipitation of the relevant metal nitrates in a potassium carbonate solution. 1 M solutions of aluminium nitrate, magnesium nitrate and nickel nitrate were prepared separately then mixed in a ratio appropriate to yield hydrotalcites of the required composition after co-precipitation. The ratio fo Ni:Mg:Al ions of the synthesised hydrotalcite was 1:1:1. A sample was also prepared with a small amount of Fe^{3+} ions in the ratio $Ni:Mg:Al^{3+}:Fe^{3+}$ of 1:1:0.7:0.3. The 1 M mixed nitrate solution was diluted to 0.1 M with deionised water then added to the carbonate solution at a rate of 5 ml min^{-1} at a temperature of 70 ^{o}C with vigorous stirring. A pH of 8.5 was maintained throughout the precipitation by the addition of 3 M sodium hydroxide from a peristaltic pump connected to a pH monitor and controller.

After the addition of the nitrate solution had ceased the hydrotalcite slurry was allowed to age, with the temperature and stirring maintained for a further 6 hours. The slurry was then filtered under vacuum and washed with five 800 ml of deionised water. The precipitate was dried in an oven in air at 65 ^{o}C for approximately 24 hours after which it was ground in an agate pestle and mortar and placed in an airtight container prior to further analysis.

2.1.2. Mixed oxide preparation

A 1g portion of the previously prepared hydrotalcite was calcined by heating in air to 600 ^{o}C at a rate of 10 ^{o}C min^{-1} and holding at that temperature for 6 hours. A change in colour from light to dark green indicated the change from hydrotalcite to mixed oxide had occurred. The surface area and textural properties were then determined by N_2 adsorption experiments.

2.1.3. Preparation of pellets for industrial application

In order to utilise hydrotalcite for industrial carbon capture applications such as pressure or temperature swing adsorption, the powdered samples must be made into pellets suitable for use in a packed bed, since powdered samples would present too high a pressure drop under a flow of gas

through the bed. Methods for manufacturing pellets include pressing, tabletting and extrusion, however the rheological properties of hydrotalcites are not favourable for extrusion unless the powder is mixed with other binders and flow aids to improve the properties of the paste, and therefore hydrotalcites were mixed with alumina prior to manufacturing the pellets. Four different hydrotalcite/alumina samples were studied, each with a different composition. For example, to make a 50 % hydrotalcite: 50 % alumina pellet, 25 g hydrotalcite samples were dry mixed with 25 g boehmite (aluminium oxide hydroxide) powder before adding 50 ml distilled water and kneading to make a paste with improved flow characteristics compared with hydrotalcite powder only. 2 g Acetic acid diluted in 10 ml of deionised water was then added in order to improve the paste rheology and impart some rigidity to the paste immediately after it has been extruded. The paste was extruded, cut into pellets of 2.5 mm diameter and 5 mm length, which were then further calcined by heating in air to 600 °C at a rate of 10 °C min^{-1} for 6 hours. After calcination, the boehmite was converted to alumina. Pellets containing different ratios of hydrotalcite : boehmite (50:50 and 70:30) were manufactured from the powdered Sample 1 and Sample 2 samples. The compositions of the hydrotalcites are given in Table 1. Some pellets were retained for future studies in a fixed bed, whilst for the purposes of thermogravimetric tests the pellets were crushed to a fine powder. For the purposes of comparison of adsorption capacities, silica gel (for flash chromatography, particle size 40-63 µm, BDH 153325P) was used as received.

2.2. Characterisation of samples

2.2.1. Nitrogen adsorption

The surface areas of the powdered mixed oxides and hydrotalcite/alumina pellets were determined by N_2 adsorption at liquid N_2 temperature using a Micromeritics ASAP 2020. The samples were first

outgassed under vacuum at 300 °C for a period of 12 hours. The average pore size was estimated from the isotherm using the BJH method on the desorption step.

Temperature programmed reduction (TPR) experiments were carried out on a Micromeritics Autochem II (2920). Approximately 50 mg of sample was used in all experiments. The samples were first held in a 10% H_2/Ar mixture flowing at 100 $cm^3\ min^{-1}$ at 100 °C for 1 hour. The temperature was then increased to 1000°C at a rate of 10 °C min^{-1} (the TPR conditions thus meeting the Malet and Caballero (1988) conditions for TPR experiments) and the hydrogen consumption recorded.

Powder X-Ray Diffraction (XRD) was carried out on the fresh hydrotalcite and mixed oxides with a Siemens D5005 diffractometer in reflection mode using CuKα radiation. The Ni^0 crystallite sizes after reduction were estimated using the Scherrer equation from the (1 1 1) reflection.

2.2.2. Thermogravimetric analysis experimental procedure

A thermogravimetric analyser (Pyris 1 TGA, PerkinElmer) was used to investigate the stability, adsorption and desorption behaviour of the hydrotalcite/alumina samples. All experiments were performed at atmospheric pressure. Dry carbon dioxide (99.8%, BOC) and nitrogen (BOC) were used as purge gas at a constant flow of circa 50 $cm^3\ min^{-1}$.

The tests were carried out for the powdered hydrotalcite samples, powdered mixed oxide, powdered boehmite, and crushed hydrotalcite/alumina pellets. A sample of 5 to 15 mg was placed in a ceramic sample pan and suspended in the furnace of the thermogravimetric analyser. A fresh sample was used for each experiment. The furnace temperature was set in the range of 20 to 600 °C according to the experimental method as described below. The temperature of the sample was measured directly under the sample pan with a thermocouple.

The following method was used to investigate the stability of the hydrotalcite/alumina at high temperatures using the thermogravimetric analyser. The samples were held at 30 °C for 2 min and then heated to 600 °C at 10 °C min^{-1}. In some experiments, subsequent cooling and re-heating cycles followed. As the cooling took much longer than the heating, a cooling rate of 50 °C min^{-1} was used

and the furnace temperature was held at 30 °C for 20 min before the next heating cycle to 600 °C at 10 °C min^{-1} was started.

The adsorption and desorption experiments were performed in the thermogravimetric analyser using the following methods. The samples were degassed and dried directly prior to the experiments. For non-calcined hydrotalcite powders the sample powder was placed in the instrument and heated to 120 °C under carbon dioxide and held for 30 minutes. It was then cooled to just above ambient temperature (25 or 20 °C) and held for 90 minutes in a flow of carbon dioxide, until the weight remained constant. Finally the sample was heated to 140 °C for 8 minutes to desorb to the initial state. The above steps were repeated to check the regeneration capability of the sample. For the mixed oxide samples, which had already been calcined, a higher temperature for the initial heating procedure of 600 °C was used, before cooling to the adsorption temperature of 25 °C.

3. Results and Discussion

3.1. Sample characterisation

3.1.1. Bet surface areas of samples

Two powdered hydrotalcite samples were prepared by a precipitation method (Sample 1 and Sample 2), and were subsequently converted into pellets suitable for use in an adsorber bed by mixing with boehmite to make a paste, extruding, drying and calcining (Samples 3-6). Boehmite is added to improve the rheological properties of the paste, resulting in the final pellet consisting of mixed hydrotalcite/alumina. Table 1 displays the compositions of each material, together with their BET surface areas determined by nitrogen sorption. Also shown for the purposes of comparison are the surface areas for boehmite powder. An isotherm obtained during the nitrogen sorption analysis is given in Fig. 1 for the mixed oxide. In all cases the adsorption/desorption experiments yielded an

isotherm closest in shape to the IUPAC type IV (Sing et al., 1985), displaying a marked hysteresis between the adsorption and desorption curves.

Isotherms of this type are characteristic of mesoporous materials, whereby the adsorption at lower values of P/P_0 is consistent with the single layer/multi layer adsorption, also found with non-porous materials, whilst the distinct hysteresis at higher values of P/P_0 indicates capillary condensation in the mesopores. The hysteresis is closest in shape to the H3 type (Sing et al., 1985). This type of hysteresis is reported to be consistent with 'slit-shaped' pores formed by aggregates of plate-like particles (Carrado et al., 2002). It is reasonable to expect that a mixed oxide derived from a hydrotalcite would display an isotherm and hysteresis of this type given the layered structure of the hydrotalcite from which it is derived.

The surface areas for the hydrotalcite powders show that the NiMgAl hydrotalcite (Sample 1) has a higher surface area than the iron containing Sample 2. These two samples were compared since there are suggestions in the literature that adding iron to the catalyst may improve its performance in the methane dry reforming reaction (Courson et al., 2000). Possibly, during heating to 300 °C for evacuation in the BET measurement, some of the hydrotalcite structure could have been destroyed and the mixed oxide formed. The surface areas and pore sizes obtained for the hydrotalcites are interesting when compared to other published data. For similar compositions they are in broad agreement with other published work, which report surface areas of between 150-200 m^2g^{-1} (Perez-Lopez et al., 2006) or exceptionally as high as 300 m^2g^{-1} when ultrasound is used during synthesis (Climent et al., 2004). Boehmite has a significantly higher surface area than hydrotalcite. After mixing with Boehmite, forming into pellets and calcining (Samples 3-6), the surface areas all lie within the range 200 – 234 m^2g^{-1}, the 50 % hydrotalcite:50 % boehmite samples having the larger surface areas than the 70 % hydrotalcite:30 % boehmite materials. This suggests that the structures of the boehmite and hydrotalcite particles are maintained, such that the final surface area of the hydrotalcite/alumina is an average of the values recorded for each of the separate starting materials. Of the hydrotalcite powders prepared the NiMgAl (Sample 1) had the highest surface area, and

therefore was selected for further characterization as the most promising sample as a candidate adsorbent for carbon dioxide.

3.1.2. Structure of NiMgAl hydrotalcite

An XRD pattern obtained for the synthesised NiMgAl hydrotalcite (Sample 1) powder is given in Fig. 2. This pattern is consistent with ones previously published such as those by Clause et al. (1993), and is indicative of a material with a layered structure. Three relatively narrow peaks occur at low 2θ values (2θ = 11.6, 23.2, 34.8°) corresponding to the 003, 006 and 012 reflections (Cavani et al., 1991). The cell parameters can be estimated from these peaks and are calculated to be a = 3.04 Å and c = 23.30 Å and the basal spacing d = 7.77 Å.

The composition of this hydrotalcite was examined by EDX in order to compare the nominal and actual composition of the synthesised materials. The measured M^{II}/M^{III} ratio was 2, in agreement with the expected value, and the measured Ni/Mg ratio was 0.98, with expected value 1.0, also displaying good agreement, suggesting that preferential precipitation of one of the metallic constituents did not occur.

After synthesis and analysis to confirm that the prepared materials were as expected, the hydrotalcites were calcined in air at 600 °C for 6 hours. This step completely destroys the layered structure of the hydrotalcite resulting in a high surface area mixed oxide. As with the fresh hydrotalcite no dependence of structure on composition was found, a typical mixed oxide XRD trace obtained is given in Fig. 3.

It can be seen from Fig. 3 that the XRD pattern in Fig. 2 has been replaced by three diffuse peaks which indicate the presence of largely amorphous NiO, MgO and solid solutions of NiO/MgO. There are no peaks present relating to any aluminium oxide species such as spinel ($MgAl_2O_4$), as they do not crystallise at the relatively low temperature at which the calcination was carried out.

3.1.3. Reduction behavior of NiMgAl hydrotalcite

The reduction properties of the mixed oxide of the Sample 1 were determined by TPR, and the results are shown in Fig. 4. The TPR trace displays three peaks, corresponding to NiO in various states of interaction with MgO. The short broad peak occurring at the lowest temperature is associated with the reduction of segregated NiO which occurs close to these temperatures (Perez-Lopez et al., 2006; Montoya et al., 2000; Parmaliana et al., 1990). Segregated NiO has previously been observed in nickel deficient hydrotalcite derived mixed oxides, the effect of the reduction peak moving towards higher temperatures with decreasing nickel content has also been previously observed (Perez-Lopez et al., 2006; Tichit et al., 1997). A 'shoulder' peak can be observed at approximately 550 ^{o}C, this peak is likely to correspond to NiO occupying surface sites in the MgO lattice, and although not directly commented on in previous work on hydrotalcites such as that by Perez-Lopez et al. (2006), it is seen in some of their TPR traces and observed in the TPR traces of non- hydrotalcite derived Ni/Al_2O_3 catalysts prepared by the incipient wetness technique or by co-precipitation (Li and Chen, 1995). The peak occurring at the highest temperature (775 ^{o}C) corresponds to NiO interacting strongly with the MgO lattice ('bulk' NiO), this peak is a common feature of NiO/MgO solid solutions and mixed oxides.

3.2. Thermogravimetric analysis of hydrotalcite powders

Powdered hydrotalcite Samples 1 and 2 were analysed for carbon dioxide adsorption both before and after calcination, using a thermogravimetric method. Fig. 5 shows the CO_2 adsorption capacity of various hydrotalcite samples and boehmite during the first, second and third temperature cycle of heating from 30 °C to 600 °C, followed by cooling. The NiMgAl hydrotalcite (Sample 1) was observed to display the highest capacity of around 1.58 mmol CO_2 (g adsorbent)$^{-1}$. This is significantly higher than the adsorption capacity of NiMgAlFe hydrotalcite (Sample 2), which only adsorbs around 1.03 mmol CO_2 (g adsorbent)$^{-1}$. There are two possible reasons for the change in adsorption capacity. Firstly, the dispersion of nickel particles, which act as adsorption sites for carbon dioxide may be

influenced by the change of composition. Secondly, the pore size and surface area may be affected by the addition of iron, thus influencing the accessibility of carbon dioxide in to the pore structure. The Brucite-layered structure of hydrotalcites contains sheets of metal and hydroxide ions intercalated with anions and water molecules. Iron (Fe^{2+}) has a relatively large ion radius of 0.76 Å, which is larger than the ion radii of Mg^{2+} and Al^{3+} ions of 0.65 and 0.6 Å respectively (Yu et al, 2008), and therefore Fe^{2+} may be difficult to be incorporated in to the hydrotalcite lattice. Another factor is the possible formation of a spinel phase ($NiFe_2O_4$ or $FeFe_2O_4$), which is more likely with increasing iron content. Sample 1 which does not contain iron, displays a surface area 19.3 % higher than Sample 2, which has iron incorporated in its structure (Table 1), which could be due to the difficulty of incorporating iron in to the lattice as mentioned above. Similarly Yu et al (2008) observed decreases in surface area with the increase in Fe content, which they attributed to the increased fraction of the spinel phase.

The effect of calcining the sample to produce the oxide form resulted in a reduced adsorption capacity of Sample 1, but an increase in the capacity of the Sample 2. The calcination to the oxide form would be expected to destroy the Brucite-layered structure. The collapse of the structure may lead to possible loss of surface area and adsorption capacity. Tichit et al (1997) noted that a three phase model is generally proposed for calcined LDH materials, which may comprise: Al-doped NiO or MgO crystallites, Ni- or Mg-doped alumina and an aluminate spinel-type phase at the Mg(Ni)O-alumina interface. The calcination could induce the formation of both the aluminate spinel-type phase and the Mg and/or Ni-doped alumina, with the spinel phase possibly leading to less adsorption capacity than the hydrotalcite as observed for Sample 1. However, the removal of water and carbon dioxide during calcination can lead to the formation of channels and pores, which could increase the specific surface area (Yu et al., 2008), and thus increase carbon dioxide adsorption as observed for Sample 2. The adsorption capacity of boehmite of 1.3 mmol CO_2 (g adsorbent)$^{-1}$ was in a similar range as that of the hydrotalcite samples. A strong influence of the hydrotalcite composition on the adsorption capacity was reported by Hutson and Attwood (2008) who found adsorption capacities for carbon dioxide in the range of 0.4 to 3.6 mmol g^{-1} at 330 °C for a variety of hydrotalcites with

different composition. In comparison with literature values, it also has to be considered that the adsorption capacity can depend on the calcination temperature (Hutson et al., 2004). Upon repeating the temperature cycles, the amount of CO_2 adsorbed at each cycle fell by a small amount, for example the amount of CO_2 adsorbed over Sample 1 hydrotalcite in the third cycle was 17 % lower than the first cycle. This reduction could possibly be due to sintering of the hydrotalcite particles at high temperature, leading to loss of surface area with increasing number of adsorption-desorption cycles. Fig. 6 shows the rate of adsorption of CO_2 over each sample, which indicates that Sample 1 displays the fastest adsorption rate of 0.17 mmol g^{-1} min^{-1}. The rate of adsorption of CO_2 upon Sample 1 during the first cycle is markedly faster than any of the other samples, but decreases with increasing number of cycles such that at the third cycle, the rate has fallen by 44 %.

3.3. Thermal stability of hydrotalcite/alumina pellets

Hydrotalcite powders were manufactured into pellets by mixing with boehmite in ratios of 50:50 or 70:30 hydrotalcite:boehmite, before making into paste, extruding, drying and calcining. Since alumina derived from boehmite can also adsorb carbon dioxide, further detailed thermogravimetric studies were carried out on the hydrotalcite/alumina composite samples. Samples of crushed and ground hydrotalcite/alumina were heated to 600 °C (calcination temperature) at 10 °C min^{-1} both under a nitrogen and carbon dioxide atmosphere. Fig. 7 shows the resulting weight loss curves for Sample 3. They are almost identical for nitrogen and carbon dioxide atmospheres. A weight loss of approximately 10% was observed on heating from 50 to 600 °C. The weight loss was constant and smooth. This indicates there was no decomposition but rather the loss of loosely bound molecules, which can be attributed to interlayer and surface water (Hutson et al., 2004). Usually, thermogravimetric curves of hydrotalcite samples show one or two further weight loss peaks at 250-600 °C, arising from dehydroxylation and decarbonisation respectively (Hutson et al., 2004; Othman et al., 2006). These decomposition processes occur during calcination and change the structure and surface of the hydrotalcites (Perez-Lopez et al., 2006). As the samples used in this study had already

undergone calcination prior to the experiments, no such decomposition processes were observed here. This indicates that re-heating of calcined samples does not result in further modification of the hydrotalcite structure. All four hydrotalcites showed virtually the same behaviour on heating to 600 °C, as shown in Fig. 8. Thus, the composition of the hydrotalcite has no influence on the stability of the hydrotalcite structure at high temperatures. This was only thought to be valid for calcined samples, as hydrotalcites with different composition of the cations magnesium, cobalt and calcium were found to have different dehydroxylation and decarbonisation temperatures by Wang et al. (2008).

Experiments with silica gel as a standard adsorbent were performed for comparison. The sample was heated to 600 °C in carbon dioxide at 10°C min^{-1}. The result is shown in Fig. 9 and was different from the behaviour of the hydrotalcites. A step was observed in the weight curve, indicating two different stages of weight loss. Initially the evaporation of water and desorption of gas occurs in a similar manner to the hydrotalcites. At approximately 300 °C, however, a second weight loss process takes place as the slope of the weight loss curve becomes steeper again. This indicates a decomposition process in the silica gel. Similar behaviour is obtained with nitrogen as the purge gas (not shown). Thus, hydrotalcites offer increased thermal stability compared to materials such as silica gel.

Subsequent cooling and re-heating cycles were performed. The results are shown in Fig. 10 for Sample 3. During the cooling process following the first heating, the mass remains nearly constant until temperatures lower than 300 °C are reached. This behaviour differs strongly from the heating process. Below 100 °C a steep increase in mass is observed during cooling, which is probably due to adsorption of the gas on the hydrotalcite. Re-heating results in a slow loss of mass. The amount of weight lost during this re-heating cycle at 600 °C equals the amount of weight increase during the previous cooling cycle, indicating that any adsorbed gas is completely desorbed at 600 °C. Hysteresis is observed for the cooling and heating of the hydrotalcite which might indicate that the desorption process is slower than the adsorption process. However, it is also possible that the hysteresis effect is caused by a slight temperature difference between the thermocouple, which was placed directly

under the sample holder, and the sample itself, during heating and cooling. The response of the actual hydrotalcite sample temperature may be slower than that of the thermocouple, thus causing the different behaviour for heating and cooling. This possible error can be excluded in the isothermal experiments described in the following sections.

After the initial loss of water in the first heating cycle, the cooling and heating cycles are reproducible, showing again that no structural damage or decomposition occurs. The behaviour of the hydrotalcite is virtually identical for carbon dioxide and for nitrogen atmosphere (not shown), so that the hysteresis seems to be a thermal effect, independent of the gas. However, the amount of weight increase/decrease during the hysteresis is slightly higher for carbon dioxide than for nitrogen. This may be an indication for higher adsorption of carbon dioxide on hydrotalcites compared to nitrogen.

3.4. Effect of pre-treatment on carbon dioxide adsorption upon hydrotalcite/alumina pellets

Sample 3 was pre-treated at different temperatures before carbon dioxide adsorption. In all cases, the sample had been calcined at 600 °C. The pre-treatment at elevated temperature mainly ensured there was no water adsorbed on the sample. Three different pre-treatment temperatures were used: 150, 300 and 600 °C. The hydrotalcite was heated to the pre-treatment temperature for 60 min in case of 150 and 300 °C, and for 10 min in case of 600 °C, and then cooled to 20 °C for carbon dioxide adsorption. When adsorption equilibrium was reached, the hydrotalcite was re-heated for desorption.

The amount of carbon dioxide adsorbed increased with increasing pre-treatment temperature (Table 2). This is in agreement with the stability experiments which showed a high weight loss in the initial heating cycle. Obviously, any loosely bound molecules on the hydrotalcite occupy adsorption sites and hinder the adsorption of carbon dioxide. The best adsorption results were obtained with pre-treatment at 600 °C, the calcination temperature, for 10 min. Therefore this pre-treatment method was used for all further experiments.

Experiments were also performed for silica gel with different pre-treatment temperatures. Unlike the hydrotalcites, silica gel showed poorer adsorption performance upon pre-treatment at higher temperatures (Table 2). Pre-treatment at 600 °C for 10 min led to a lower adsorption of carbon dioxide at 20 °C than pre-treatment at 150 °C for 60 min. This is in line with the stability results which show some decomposition or change in structure at circa 300 °C. Therefore, the pre-treatment method at the lower temperature of 150 °C was used for silica gel in the low-temperature sorption experiments at 20 °C. For the experiments with desorption temperatures of 150 and 300°C, however, the higher pre-treatment temperature was used.

3.5. Desorption behaviour of hydrotalcite/alumina pellets

Desorption was performed in the previously described experiments by re-heating the hydrotalcite to the desorption temperature. If desorption temperature was chosen to be the same temperature as used for pre-treatment, complete desorption was observed for all the experiments (Table 2). As a temperature of 150 °C was sufficient for complete carbon dioxide desorption in the experiment with pre-treatment at 150 °C, an experiment was performed using 300 °C for pre-treatment and 150 °C for desorption. Desorption was not complete in this case, and the desorbed amount of carbon dioxide was virtually equal to the amount adsorbed and desorbed in the experiment with 150 °C as the pre-treatment and desorption temperature (Table 2). A methodical effect caused by the thermogravimetric measurement can be excluded, as temperature and buoyancy effects were checked with a non-adsorbent sample (glass beads) and proved to be negligible. Obviously high temperatures are required for complete desorption. This may show that chemisorption is involved. Note, however, that desorption in these experiments was carried out in the same gas atmosphere as the adsorption. Thus, desorption was driven merely by the change in temperature and consequent change of the adsorption equilibrium. Complete desorption was obtained for all further experiments on heating to 600 °C. Therefore, complete desorption can be achieved at high temperatures even in the atmosphere of the adsorbed gas. At lower pressure, it would certainly be possible to use lower

temperatures for desorption. Adsorption at lower temperatures may also be performed with nitrogen at atmospheric pressure, but some nitrogen adsorption can occur in this case.

3.6. Comparison of carbon dioxide adsorption capacity upon hydrotalcite/alumina pellets

Fig. 11 shows the adsorbed amount of carbon dioxide on the hydrotalcite/alumina samples with variation of temperature. The results for silica gel are included in the graph for comparison. Adsorption decreases with increasing temperature, again showing virtually the same adsorption capacities for all four hydrotalcites. The overall amount of carbon dioxide adsorbed is higher than some reported studies (Choi et al., 2009). One reason is that in this study the lowest temperature at which adsorption was measured was 25 °C, whereas in the survey of Choi et al. (2009), the lowest temperature was 473 K, (200 °C). The decreasing adsorption with increasing temperature is in accordance with literature results (Othman et al., 2006), whereas a maximum adsorption was found at a temperature of 300 °C by Yong et al. (2002). It is noted that the results presented in Fig. 11 refer to dry carbon dioxide. In the presence of water vapour, adsorption capacities of hydrotalcites is expected to markedly increase.

There is no significant difference in the adsorption between the four different hydrotalcite/alumina samples at 150 and 300 °C. At 20 °C, Sample 6 shows a slightly higher adsorption and Sample 3 a slightly lower adsorption than the other hydrotalcites in this study. However, this small difference may arise from the experimental inaccuracy due to small differences in sample mass. From the results obtained in this study, no general trends can be seen and the adsorption seems to be independent of the hydrotalcite composition. Additionally, mixing the hydrotalcite with boehmite and calcining at 600 °C would have lead to a different structure to non-calcined hydrotalcite, incorporating particles of mixed oxide within an alumina matrix. It may be the case that some adsorption occurs over the alumina with which hydrotalcite is mixed during pellet manufacture. In that case, the composition of the hydrotalcite itself has less influence upon the

adsorption capacity compared with the pure non-calcined hydrotalcite, as reported in the literature (Hutson et al., 2008; Yong et al., 2002).

Carbon dioxide adsorption on the hydrotalcites is more than twice as high as the adsorption on silica gel under the same conditions. This shows that hydrotalcites are indeed a suitable sorbent for carbon dioxide over a wide temperature range. At 20 °C, adsorption of carbon dioxide is between 2.0-2.5 mmol g^{-1} for all the hydrotalcite samples in this study. Yong et al. (2002), reported adsorption capacities for carbon dioxide between 0.1-0.25 mmol g^{-1} for different hydrotalcite samples at 25 °C. An adsorption capacity of approximately 0.25 mmol g^{-1} was also found by Soares et al. (2005) at 29 °C for a hydrotalcite containing only Mg and Al as cations. In comparison, the hydrotalcites used in this study, containing different amounts of Ni and Fe, show increased carbon dioxide adsorption capacity at low temperatures. Although the adsorption capacity decreases at higher temperatures, the hydrotalcites still show higher adsorption capacity for carbon dioxide than, for example, silica gel. Amine modified functionalised SBA-12 meso-porous silicas showed adsorption capacities for carbon dioxide of up to 1.4 mmol g^{-1} (Zelenak et al., 2008). Carbon dioxide adsorption capacities of 0.25-0.5 mmol g^{-1} at 300 °C and 0.1-0.9 mmol g^{-1} at 200 °C (Hutson et al., 2004; Yong et al., 2002) have been reported for hydrotalcites. The results reported in this work for hydrotalcites containing Ni and Fe as cations are in the same range range, with 0.6 mmol g^{-1} at 150 °C and 0.2 mmol g^{-1} at 300 °C respectively.

3.7. Long-term sorption behaviour

In order to check the long-term sorption behaviour of the hydrotalcite/alumina pellet samples, several sorption experiments were performed with the same sample (Sample 3), at an elevated temperature of 150 °C, since the hydrotalcites would be exposed to higher temperatures during service in a carbon capture unit. After the first adsorption-desorption cycle the sample was allowed to cool. Another adsorption-desorption cycle was then carried out with the same sample using the

same experimental procedure including pre-treatment. The results are shown in Table 3. The adsorption was slightly lower for the used sample than for the fresh sample. This decrease in adsorption capacity was reproducible. It is possible that although desorption seems to be complete, some chemisorption occurs which leads to blocking of adsorption sites for subsequent adsorption cycles. However the loss in adsorption capacity of the second cycle for the calcined hydrotalcite/alumina samples was much lower than for the hydrotalcite powders, shown in Fig. 5. A slight initial decrease in adsorption capacity over several cycles has also been reported by several research groups (Hutson and Attwood, 2004; Oliveira et al., 2008; Yong et al., 2002), whereas Ebner et al. (2007) found a constant sorption behaviour over many cycles.

3.8. Effect of sample morphology

The effect of the sample morphology on the adsorption of carbon dioxide on a hydrotalcite sample was investigated. In this case, the hydrotalcite sample was used in pellet form rather than crushed to a fine powder. The result is shown in Table 3. The adsorption of carbon dioxide on the pellet was slightly lower than on the powder. More surface and possibly more pores are accessible in the powder than in the pellet, which is crucial for adsorption. Furthermore, mass transport limitations are minimised for the powder compared to the pellet. If hydrotalcites are used in a post-combustion adsorber, an optimum particle size has to be found, as a fine powder increases the pressure drop in a packed bed. In order to make a detailed assessment of the effect of particle size, both external and internal diffusion at the pellet have to be considered (Seader and Henley, 1998). For external diffusion, the mass transfer coefficient can be determined from the Sherwood number, which is correlated with Reynolds and Schmidt numbers (Ranz and Marshall, 1952):

$$Sh = 2 + 0.6Sc^{1/3}\,\mathrm{Re}^{1/2} \quad (1)$$

From this equation, it can be deduced that at high Reynolds numbers above 2000, where $2 << 0.6Sc^{1/3}\,\mathrm{Re}^{1/2}$, the mass transfer coefficient k_c is proportional to $d_p^{-1/2}$. Thus increasing the

particle size will have the effect of reducing the mass transfer coefficient and increasing external diffusion limitations. To analyze internal diffusion within the pellet, the concentration of carbon dioxide, C, as a function of the pellet radius, r, may be calculated by solving the following equation with appropriate boundary conditions:

$$D_e\left(\frac{\partial^2 C}{\partial r^2}+\frac{2}{r}\frac{\partial C}{\partial r}\right)=\frac{\partial q}{\partial t} \qquad (2)$$

where q is the amount adsorbed per unit volume of the porous pellet and D_e is the effective diffusivity in the pellet. The effective diffusivity is comprised of contributions from bulk and Knudsen diffusion in the gas phase and surface diffusion of adsorbed molecules upon the pore walls of the pellet. The internal pore structural parameters of porosity and tortuosity also influence the value of D_e (Seader and Henley, 1998). The use of smaller particles leads to reduced internal diffusion resistance, however in a fixed bed reactor the pressure drop, calculated from the Ergun equation, is higher for smaller particles. Therefore a trade-off in selecting the optimum particle size occurs, where the particular optimum may be specific to certain adsorber designs or conditions. Typical adsorbent pellet effective diameters for gas phase applications are around 2-5 mm. Detailed designs and modelling of adsorbers for these hydrotalcites will be the subject of future investigations.

3.9. Strategies for integration of adsorption processes in carbon capture and storage processes

Application of adsorbents, amongst other possible technologies, within carbon capture and storage plants could provide a means of reducing carbon emissions from large scale point source such as power stations. Such technologies are part of a portfolio of measures to try to limit or reduce the effects of climate change (Chalmers et al., 2009). Carbon capture processes can be classified into one of three categories (Penht and Henkel, 2009):

- *Post combustion capture,* involves the separation of carbon dioxide in the flue gases from other components.

- *Pre combustion capture*, in which the fuel for the power plant is converted into carbon dioxide and hydrogen then separating the carbon dioxide from hydrogen, the latter of which is burnt in the boilers.
- *Oxyfuel*, where the combustion air is first separated into nitrogen and oxygen, such that the fuel can be burnt is pure oxygen, giving a flue gas of carbon dioxide and water vapour, from which purified carbon dioxide is easily separated.

Although currently absorption into liquids is favoured for pre and post combustion carbon capture, adsorption on to solid materials could avoid the handling and regeneration of potentially environmentally damaging solvents. For pre-combustion capture, where gas is at high pressure, the most suitable capture process is pressure-swing adsorption. However, in post combustion capture, the low pressure of the flue gas favours temperature swing adsorption. Therefore any adsorbent used for post combustion capture must be capable of operating at elevated temperature, for example up to 75 °C (Arenillas et al., 2005). Choi et al. (2009) reviewed the available types of adsorbents and concluded that physisorbents such as carbons and zeolites show better adsorption capacity and selectivity close to ambient temperatures. Chemisorbents such as metal oxides and hydrotalcites are able to be used up to higher temperatures (573-673 K respectively), but on the other hand can be more difficult to regenerate. Ongoing development of specialised adsorbents such as supported amines has led to higher adsorptive capacities, but their use may be limited to lower temperatures to avoid damaging the amine groups. The selection of a suitable adsorbent will depend on many factors including the adsorptive capacity, ease of regeneration, lifetime, cost and stability under process conditions.

4. Conclusions

Hydrotalcites are suitable sorbents for carbon dioxide over a wide temperature range. Although adsorption is much better at low temperatures, hydrotalcites still possess advantages over other

sorbents such as silica gel at high temperatures. Unlike silica gel, hydrotalcite is stable at high temperatures and still has a fairly good adsorption capacity for carbon dioxide. Prior to combination with boehmite and calcination, the hydrotalcites showed some effect of composition upon carbon dioxide uptake, with Sample 1 displaying the highest capacity and adsorption rate. However, the effect of composition upon carbon dioxide adsorption decreased upon combining with boehmite and calcining to make pellets. Ongoing testing will be used to confirm the selectivity of adsorption of carbon dioxide from mixed carbon dioxide/nitrogen gas streams, and will include humid gases under flow conditions in a fixed bed reactor. Further development of hydrotalcites could focus on intercalation of the Brucite layers with carbon dioxide accepting organic molecules such as calixarenes or attachment of basic functional groups such as amines to their surface, in order to further enhance their capability for carbon dioxide adsorption. The studies reported here with standard hydrotalcite samples measured by TGA under dry conditions will thus provide a useful benchmark for comparison with future studies modified adsorbents.

Acknowledgements

EPSRC funding is gratefully acknowledged from the "C-Cycle" project EP/010601/1 (Birmingham) and EP/E010318/1 (Sheffield).

Nomenclature

a	Unit cell dimension in the x-direction, determined by XRD (Å)
c	Unit cell dimension in the z-direction, determined by XRD (Å)
C	Concentration of solute (kg m^{-3})
d	*d*-spacing, the interatomic spacing, determined by XRD (Å)
d_p	Particle diameter (m)
D_e	Effective diffusivity in a pellet (m^2s^{-1})

1	D_i	Diffusivity of component i ($m^2 s^{-1}$)
2	k_c	Mass transfer coefficient ($m\ s^{-1}$)
3	M	Metal ion
4	q	Amount adsorbed per unit volume of pellet ($kg\ m^{-3}$)
5	r	Pellet radius (m)
6	Re	Reynolds number $\mathrm{Re} = \rho u d_p / \mu$
7	Sc	Schmidt number $Sc = \mu / \rho D_i$
8	Sh	Sherwood number $Sh = k_c d_p / D_i$
9	t	Time (s)
10	u	Fluid velocity ($m\ s^{-1}$)
11	μ	Dynamic viscosity ($N\ s\ m^{-2}$)
12	θ	Diffraction angle of XRD (degrees)
13	ρ	Fluid density ($kg\ m^{-3}$)
14		
15		

References

Arenillas, A., Smith, K.M., Drage, T.C., Snape, C.E., 2005, CO_2 capture using some fly ash-derived carbon materials. Fuel, 84: 2204 – 2210.

Barriga, C., Fernandez, J.M., Ulibarri, M.A., Labajos, F.M. and Rives, V., 1996, Synthesis and characterization of new hydrotalcite-like compounds containing Ni(II) and Mn (III)_in the hydroxide layers and of their calcination, J Solid State Chem, 124: 205 – 213.

Bhattacharyya, A., Chang, V.W. and Schumacher, D.J., 1998, CO2 reforming of methane to syngas I: evaluation of hydrotalcite clay-derived catalysts, Appl Clay Sci 12:317 – 328.

Bhattacharyya, A. and Hall, D.B., New triborate-pillared hydrotalcites, 1992, Inorganic Chem, 31, 3869 – 3870.

Carja, G., Nakamura, R., Aida, T, Niiyama, H., 2001, Textural properties of layered double hydroxides: effect of magnesium substitution by copper or iron, Micropor Mesopor Mat, 47: 275 – 284.

Carpani, I., Berrettoni, M., Ballarin, B., Giorgetti, M., Scavetta, E., Tonelli, D., 2004, Study on the intercalation of hexacyanoferrate(II) in a Ni, Al based hydrotalcite, Solid State Ionics, 168: 167-175.

Carrado, K.A., Csencsits, R., Thiyagaragjan, P, Seifert, S., Macha, S.M., Harwood, J.S., 2002, Crystallization and textural porosity of synthetic clay minerals, Mater Chem, 12: 3228 – 3237.

Cavani, F., Trifiro, F. and Vaccari, A., 1991, Hydrotalcite-type anionic clays: preparation, properties and applications, Catal Today 11: 173 – 301.

Chalmers, H., Jakeman, N., Pearson, P., Gibbins, J., 2009, Carbon capture and storage deployment in the UK: what next after the UK government's competition? Proc. IMechE 223 Part A:305 – 319.

Chmielarz, L., Kustrowski, P., Rafalska-Lasocha, A., Majda, D., Dziembaj, R., 2002, Catalytic activity of Co-Mg-Al, Cu-Mg-Al and Cu-Co-Mg-Al mixed oxides derived from hydrotalcites in SCR of NO with ammonia. Appl Catal B, 35: 195 - 210.

Choi, S., Drese, J.H. and Jones, C.W., 2009, Adsorbent materials for carbon dioxide capture from large anthropogenic point sources. Chem Sus Chem, 2: 796 – 854.

Clause, O., Goncalves Coelho, M., Gazzano, M.,Matteuzzi, D., Trifirò, F. and Vaccari, A., 1992, Synthesis and thermal reactivity of nickel-containing anionic clays, Appl Clay Sci, 8: 169 – 186.,

Climent, M.J., Corma, A., Iborra, S., Epping, K., and Velty, A., 2004, Increasing the bascity and catalytic activity of hydrotalcites by different synthesis procedures, J Catal, 225: 316 – 326.

Costantino, U., Marmottini, F., Nocchetti, M., Vivani, R., 1998, New synthetic routes to hydrotalcite-like compounds – Characterisation and properties of the obtained materials, Europ J Inorg Chem: 1439-1446.

Courson, C., Makaga, E., Petit, C., Kiennemann, A., 2000, Development of Ni catalysts for gas production from biomass gasification. Reactivity in steam- and dry-reforming, Catal Today, 63: 427 – 437.

Ebner, A.D., Reynolds, S.P. and Ritter, J.A., 2007, Nonequilibrium kinetic model that describes the reversible adsorption and desorption behavior of CO2 in a K-promoted hydrotalcite-like compound, Ind Eng Chem Res, 46, 1737 – 1744.

Huang, H.Y., Yang, R.T., Chinn, D., Munson, C.L., 2003, Amine-grafted MCM-48 and silica xerogel as superior sorbents for acidic gas removal, Ind Eng Chem Res , 42: 2427 – 2433.

Hutson, N.D. and Attwood, B.C., 2008, High temperature adsorption of CO2 on various hydrotalcite-like compounds, Adsorption, 14: 781 – 789.

Hutson, N.D., Speakman, S.A. and Payzant, E.A., 2004, Structural effects on the high temperature adsorption of CO2 on a synthetic hydrotalcite. Chem Mater, 16: 4135 – 4143.

Kloprogge, J.T., Hickey, L., Frost, R.L., 2005, The effect of varying synthesis conditions on zinc chromium hydrotalcite: a spectroscopic study, Mater Chem Phys, 89: 99 – 109.

Intergovernmental Panel on Climate Change, IPCC Fourth Assessment Report (AR4), 2007, http://www.ipcc.ch/.

Li, C., and Chen, Y.W., 1995, Temperature-programmed-reduction studies of nickel oxide/alumina catalysts: effects of the preparation method, Thermochim Acta, 256, 457 – 465.

Lwin, Y. and Abdullah, F., 2009, High temperature adsorption of carbon dioxide on Cu-Al hydrotalcite-derived mixed oxides: kinetics and equilibria by thermogravimetry, Journal of Thermal Analysis and Calorimetry, 97: 885 – 889.

Majchrzak-Kuceba, I. and Nowak, W., 2005, A thermogravimetric study of the adsorption of CO2 on zeolites synthesized from fly ash, Thermochimica Acta, 437: 67 – 74.

Malet, P. and Caballero, A., 1988, The selection of experimental conditions in temperature-programmed reduction experiments, J Chem Soc Faraday Trans I, 84: 2369-2375.

Montoya, J.A., Romero-Pascual, E., Gimon, C., Del Angel, P., Monzon, A., 2000, Methan reforming with CO2 over Ni/ZrO2-CeO2 catalysts prepared by sol-gel, Catal Today, 63: 71-85.

Mosqueda, H.A., Vaquez, C., Bosch, P and Pfeiffer, H., 2006, Chemical sorption of carbon dioxide (CO2) on lithium oxide (Li2O), Chem Mater 18: 2307 – 2310.

Ohishi, Y., Kawabata, T., Shishido, T., Takaki, K., Zhang, Q.H., Wang, Y., Nomura, K., and Takehira, 2005, Mg-Fe-Al mixed oxides with mesoporous properties prepared from hydrotalcite as precursors: Catalytic behavior in ethylbenzene dehydrogenation, Appl Catal A, 288, 220 – 231.

Olafsen, A., Slagern, A., Dahl, I.M., Olsbye, U., Schuurman, Y., Mirodatos, C., 2005, Mechanistic features for propane reforming by carbon dioxide over a Ni/Mg(Al)O hydrotalcite-derived catalyst, J Catal, 229: 163 – 175.

Oliveira, E.L.G., Grande, C.A. and Rodrigues, A.E., 2008, CO2 sorption on hydrotalcite and alkali-modified (K and Cs) hydrotalcites at high temperatures, Sep Purific Technol, 62: 137 – 147.

Othman, M.R., Rasid, N.M., Fernando, W.J.N., 2006, Mg-Al hydrotalcite coating on zeolites for improved carbon dioxide adsorption, Chem Eng Sci, 61: 1555-1560.

Parmaliana, A., Arena, F., Frusteri, G., Giordano, N., 1990, Temperature-programmed reduction study of NiO-MgO Interactions in magnesia-supported Ni catalysts and NiO-MgO physical mixture, J Chem Soc Faraday T, 86: 2663-2669.

Pehnt, M. and Henkel, J., 2009, Life cycle assessment of carbon dioxide capture and storage from lignite power plants, International Journal of Greenhouse Gas Control, 3: 49 – 66.

Perez-Lopez O.W., Senger, A., Marcilio, N.R., Lansarin, M.A., 2006, Effect of composition and thermal pretreatment on properties of NiMgAl catalysts for CO2 reforming of methane, Appl Catal A , 303:234-244.

Radosz, M., Hu, X.D., Krutkramelis, K., Shen, Y.Q., 2008, Flue-gas carbon capture on carbonaceous sorbents: Toward a low cost multifunction carbon filter for “green” energy producers, Ind Eng Chem Res, 47: 3783 – 3794.

Ranz, W.E. and Marshall, W.R., 1952, Evaporation from drops 2, Chem Eng Prog 48: 173 – 180.

Roesch, A., Reddy, E.P., Smirniotis, P.G., 2005, Parametric study of Cs/CaO sorbents with respect to simulated flue gas at high temperatures, Ind Eng Chem Res, 44: 6485 – 6490.

Seader, J.D. and Henley, E.J., 1998, Separation Process Principles, Chapter 15, (John Wiley and Sons, New York, USA), pp 812-818.

Sing, K.S.W., Everett, D.H., Haul, R.A.W., Moscou, L., Pierotti, R.A., Rouquerol, J., Siemieniewska, T., 1985, Reporting physisorption data for gas solid systems with special reference to the determination of surface area and porosity (recommendations 1984), Pure Appl Chem, 57: 603 – 619.

Soares, J.L., Casarin, G.L., Jose, H.J., Moreira, R.D.F.P.M., 2005, Experimental and theoretical analysis for the CO2 adsorption on hydrotalcite, Adsorption, 11: 237 – 241.

Takehira, K., Shishido, T., Wang, P., Kosaka, T. and Takaki, K., 2003, Steam reforming of CH4 over supported Ni catalysts prepared from a Mg-Al hydrotalcite-like anionic clay. Phys Chem Chem Phys, 5: 3801 – 3810.

Tamura, H., Chiba, J., Ito, M., Takeda, T., Kikkawa, S., 2004, Synthesis and characterization of hydrotalcite-ATP intercalates, Solid State Ionics, 172, 607 – 609.

Tichit, D., Medina, F., Coq, B. and Dutartre, R., 1997, Activation under oxidizing and reducing atmosphere of Ni-containing layered double hydroxides, Appl Catal A, 159: 241 – 258.

Tsyganok, A.I., Tsunoda, T., Hamakawa, S., Suzuki, K., Takehira, K., Hayakawa, T., 2003, Dry reforming of methane over catalysts derived from nickel-containing Mg-Al layered double hydroxides, J Catal, 213: 191 – 203.

Unnikrishnan, R. and Narayanan, S., 1999, Metal containing layered double hydroxides as efficient catalyst precursors for the selective conversion of acetone, J Mol Catal A, 144: 173 – 179.

Walspurger, S., Boels, L., Cobden, P.D., Elzinga, G.D. Haije, W.G., van den Brink, R.W., 2008, The crucial role of the K+-aluminium oxide interaction in K+-promoted alumin- and hydrotalcite-based materials for CO2 sorption at high temperatures, Chem Sus Chem, 1: 643 – 650.

Wang, X.P., Yu, J.J., Cheng, J., Hao, Z.P. and Xu, Z.P., 2008, High-temperature adsorption of carbon dioxide on mixed oxides derived from hydrotalcite-like compounds, Environmental Science and Technology, 42:614 – 618.

Wang, Y. and Levan, M.D., 2009, Adsorption equilibrium of carbon dioxide and water vapor on zeolites 5A and 13X and silica gel: pure components, J Chem Eng Data, 54: 2839 – 2844.

Yong, Z., Mata, V. and Rodrigues, A.E., 2002, Adsorption of carbon dioxide at high temperature – a review, Sep Purif Technol, 26: 195 – 205.

Yong, Z. and Rodrigues A.E., 2002, Hydrotalcite-like compounds as adsorbents for carbon dioxide, Energy Conversion and Management, 43: 1865 – 1876.

Yu, Z. Chen, D., Ronning, M., Torbjorn, V., Ochoa-Fernández, E., Holmen, A., 2008, Large-scale synthesis of carbon nanofibers on Ni-Fe-Al hydrotalcite derived catalysts. I. Preparation and characterization of the Ni-Fe-Al hydrotalcites and their derived catalysts, Appl Catal A, 338: 136 – 146.

Zelenak, V., Halamova, D., Gaberova, L., Bloch, E., Llewellyn, P, 2008, Amine-modified SBA-12 mesoporous silica for carbon dioxide capture: Effect of amine basicity on sorption properties, Micropor and Mesopor Mat, 116: 358 – 364.

List of Figure and Table Captions

Fig. 1. A BET adsorption isotherm for the mixed oxide prepared by calcining NiMgAl (Sample 1) hydrotalcite in static air at 600^{o}C for 6 hours

Fig. 2. Powder XRD trace of the synthesised NiMgAl (Sample 1) hydrotalcite

Fig. 3. Powder XRD trace of the mixed oxide prepared by the calcination of Sample 1

Fig. 4. TPR traces for the NiMgAl (Sample 1) hydrotalcite derived mixed oxide

Fig. 5. Comparison of adsorption capacity of hydrotalcites, mixed oxides and boehmite powders, measured by TGA at 25 °C.

Fig. 6. Specific rate of adsorption for hydrotalcites, mixed oxides and boehmite powders, measured by TGA at 25 °C.

Fig. 7. Thermogravimetric analysis of Sample 3 in carbon dioxide and nitrogen on heating from 30 to 600 °C at a heating rate of 10 °C min^{-1}.

Fig. 8. Thermogravimetric analysis of hydrotalcite Samples 3 - 6 in carbon dioxide on heating from 30 to 600 °C at a heating rate of 10 °C min^{-1}.

Fig. 9. Thermogravimetric analysis of silica gel in carbon dioxide on heating from 30 to 600 °C at a heating rate of 10 °C min^{-1}.

Fig. 10. Thermogravimetric analysis of Sample 3 in carbon dioxide on heating from 30 to 600 °C at a heating rate of 10 °C min^{-1} with two subsequent cooling and re-heating cycles.

Fig. 11. Adsorption of dry carbon dioxide on hydrotalcites (Samples 3 -6) and silica gel as a function of temperature at atmospheric pressure and 100% CO_2 atmosphere.

Table 1. A comparison of the surface area and textural properties of various hydrotalcite derived mixed oxides. Samples 1 and 2 were used in non-calcined form. Samples 3 – 6 were calcined at 600 °C in air.

Table 2. Adsorption and desorption of carbon dioxide at different pre-treatment and desorption temperatures; Sample 3 was calcined at 600 °C

Table 3. Adsorption of carbon dioxide on Sample 3 at 150 °C under different sample conditions

Figure 1
Click here to download high resolution image

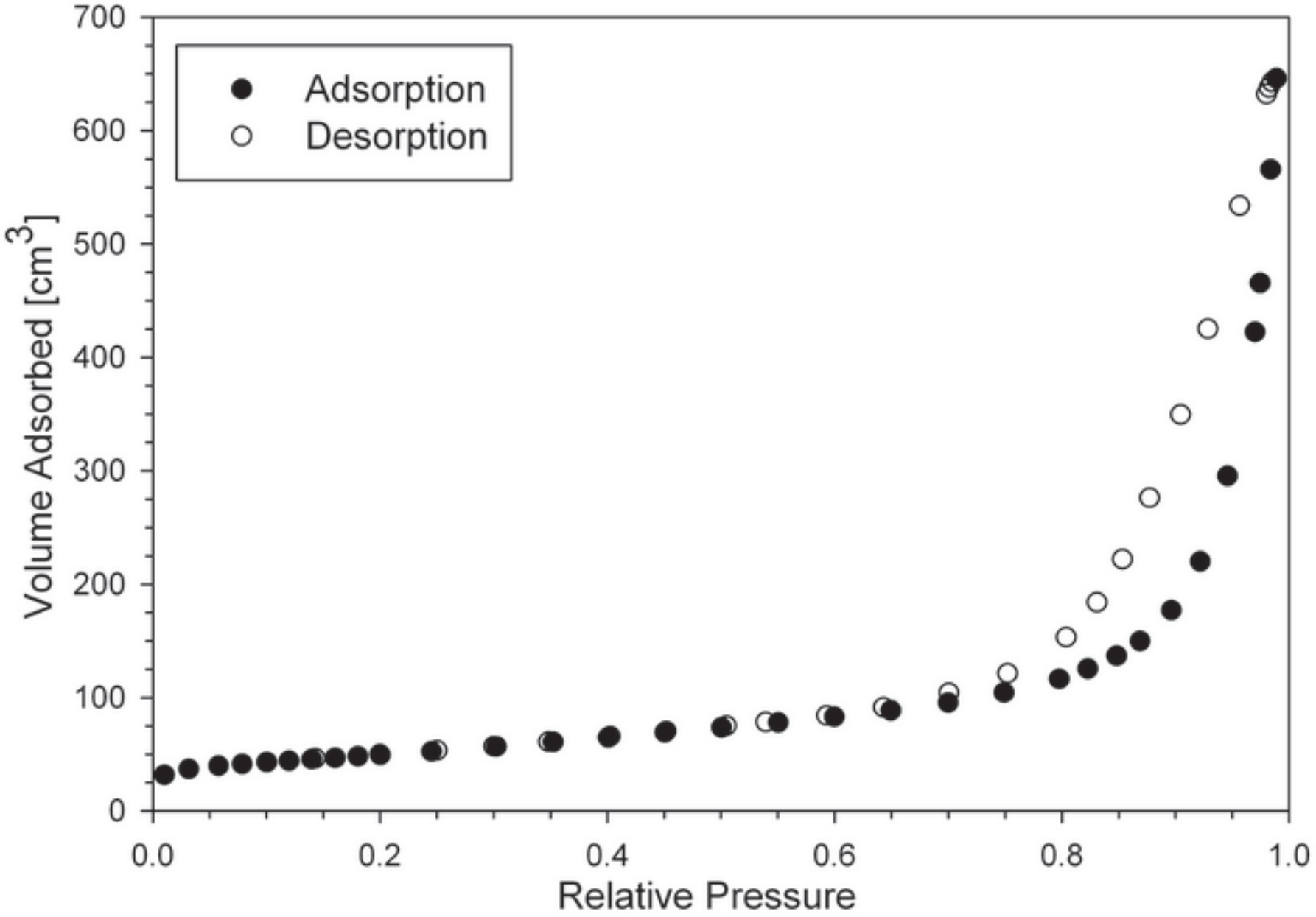

Figure 2
Click here to download high resolution image

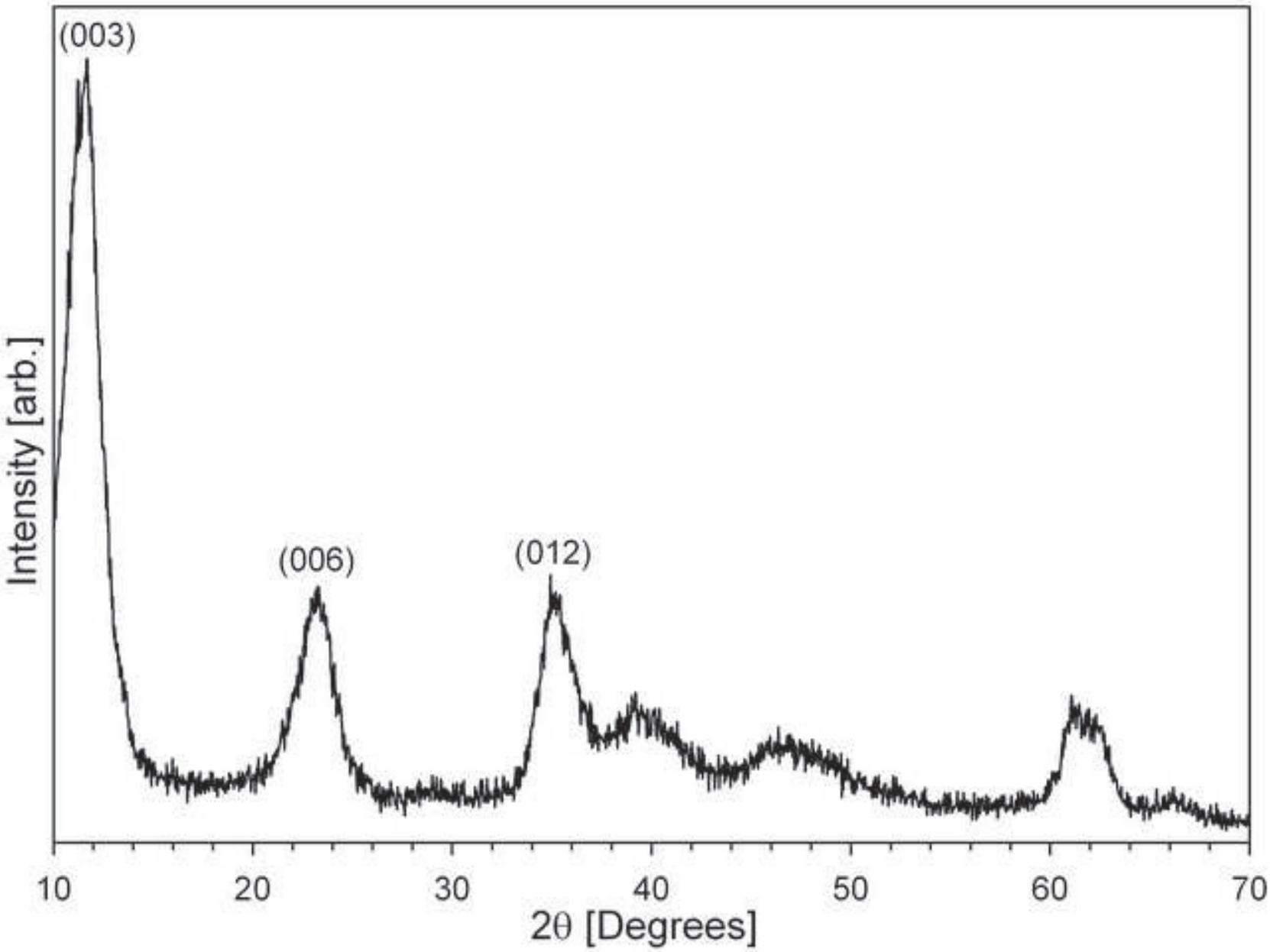

Figure 3
Click here to download high resolution image

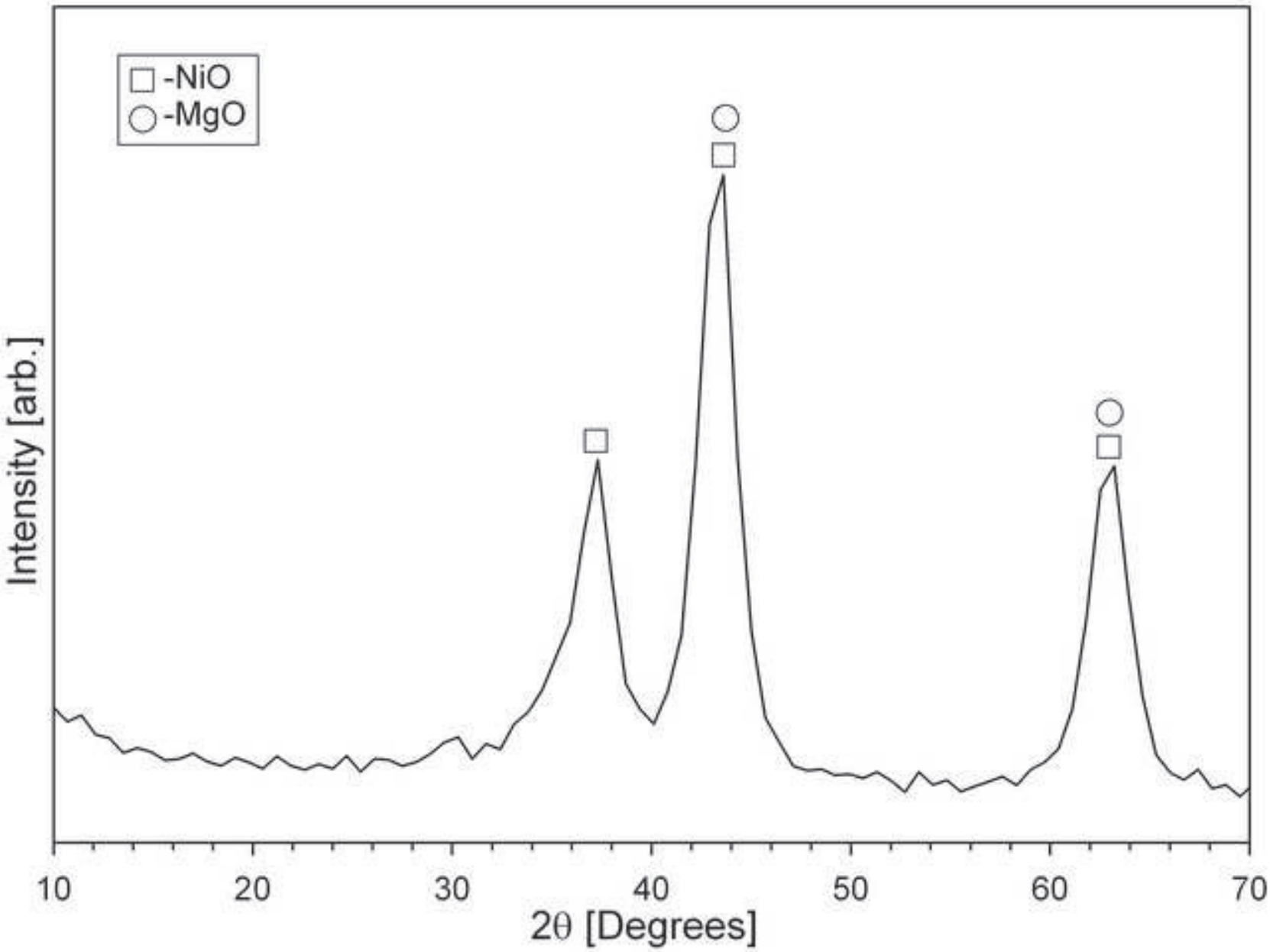

Figure 4
Click here to download high resolution image

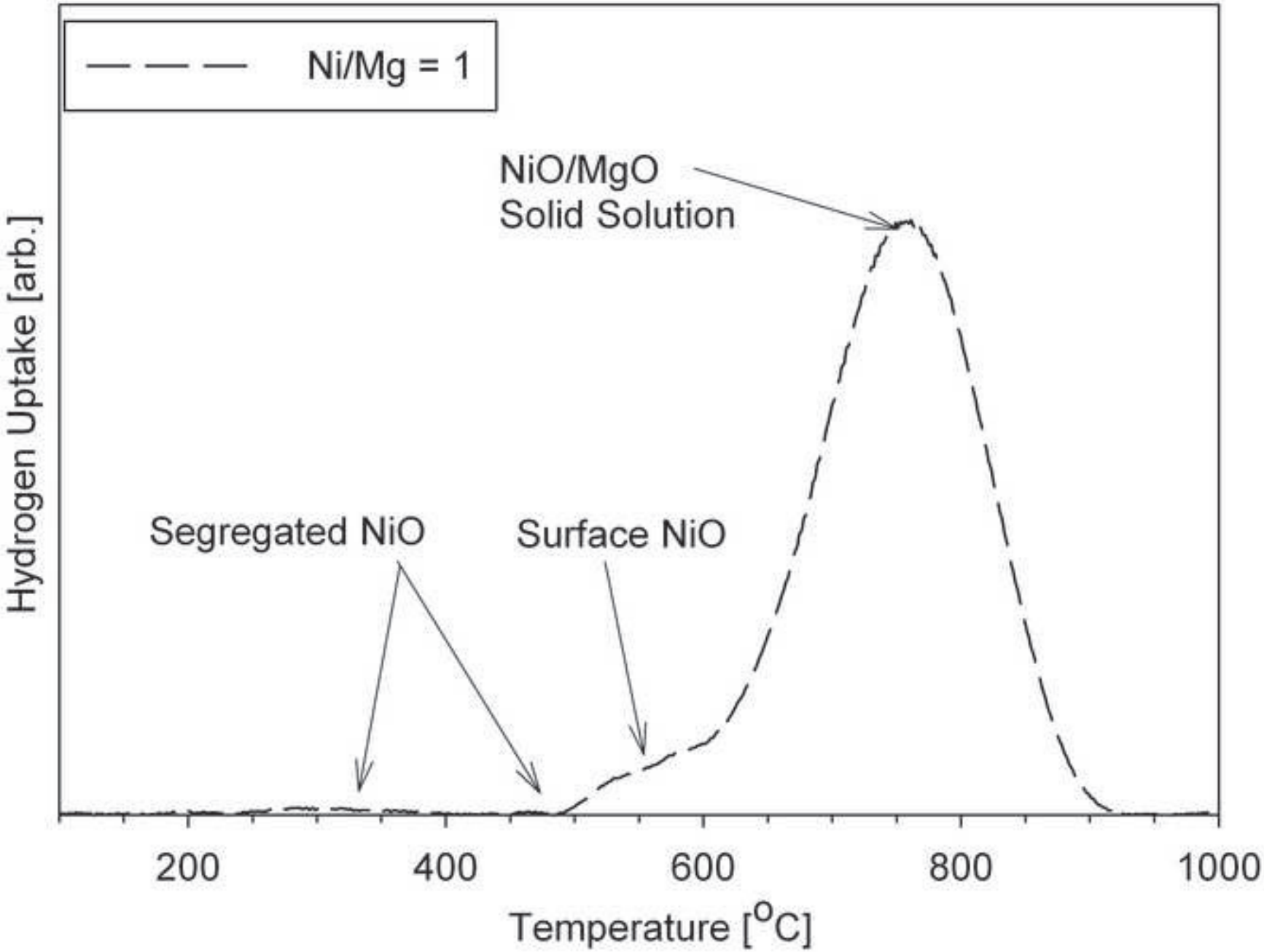

Figure 5
Click here to download high resolution image

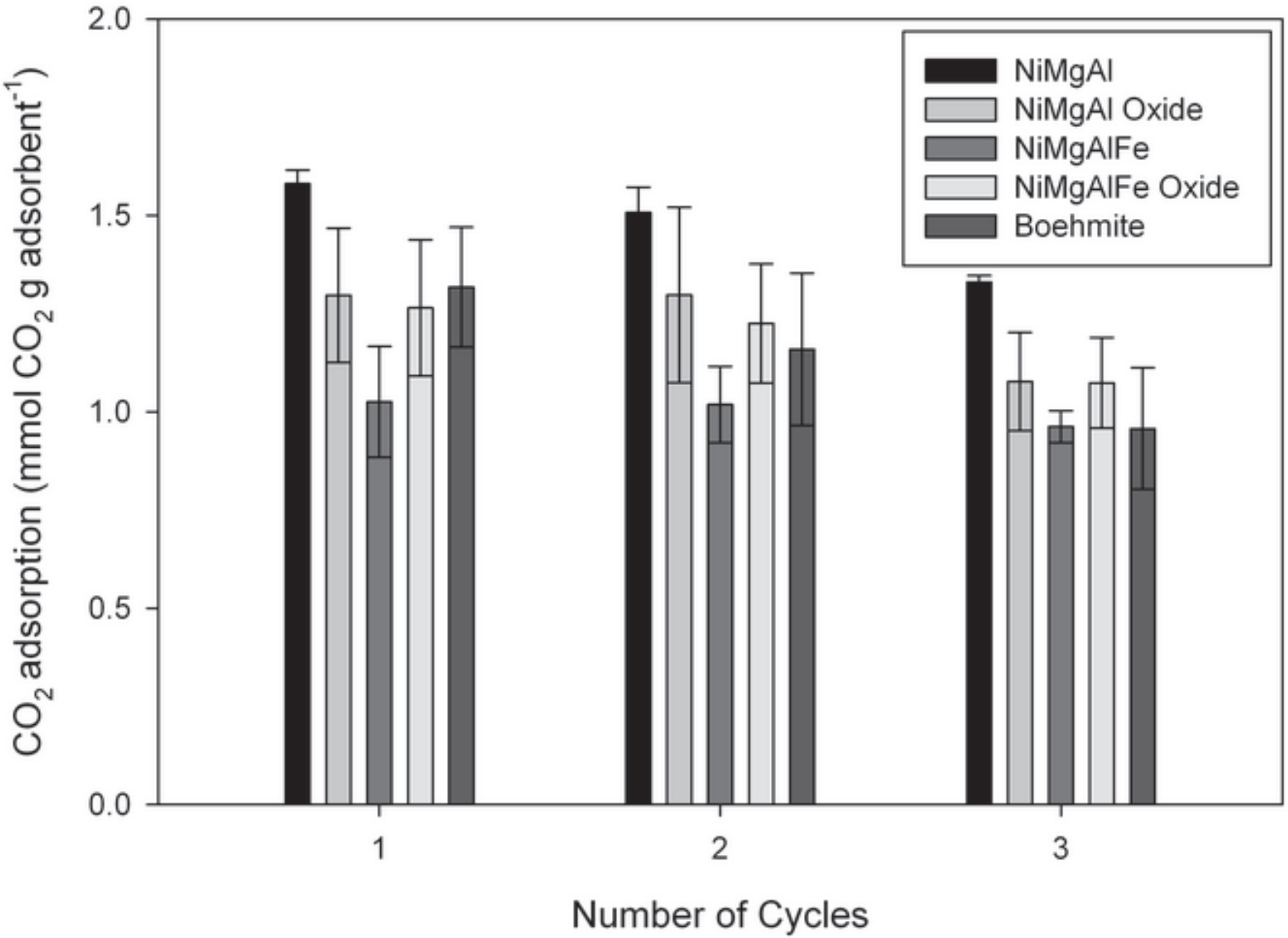

Figure 6
Click here to download high resolution image

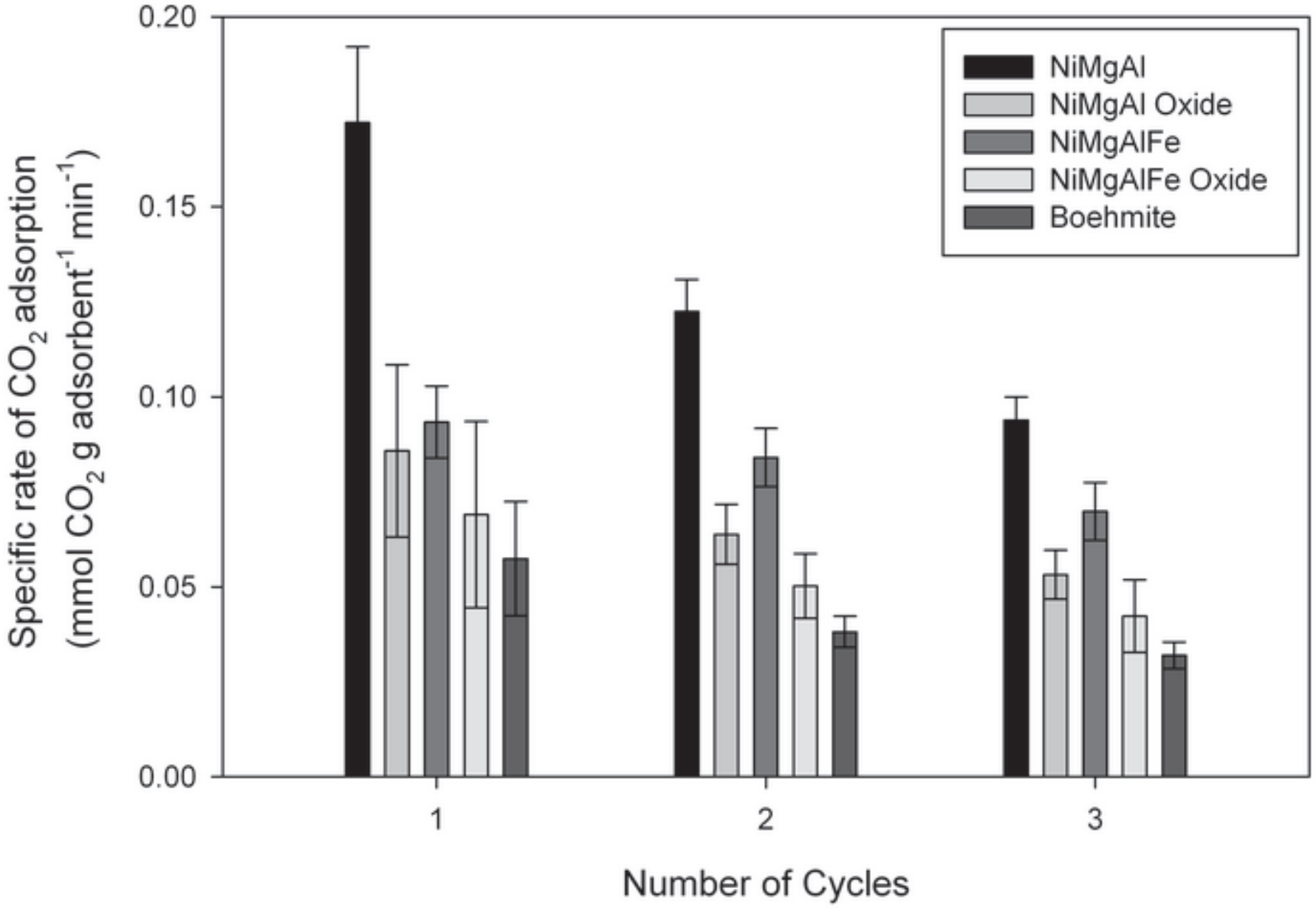

Figure 7
Click here to download high resolution image

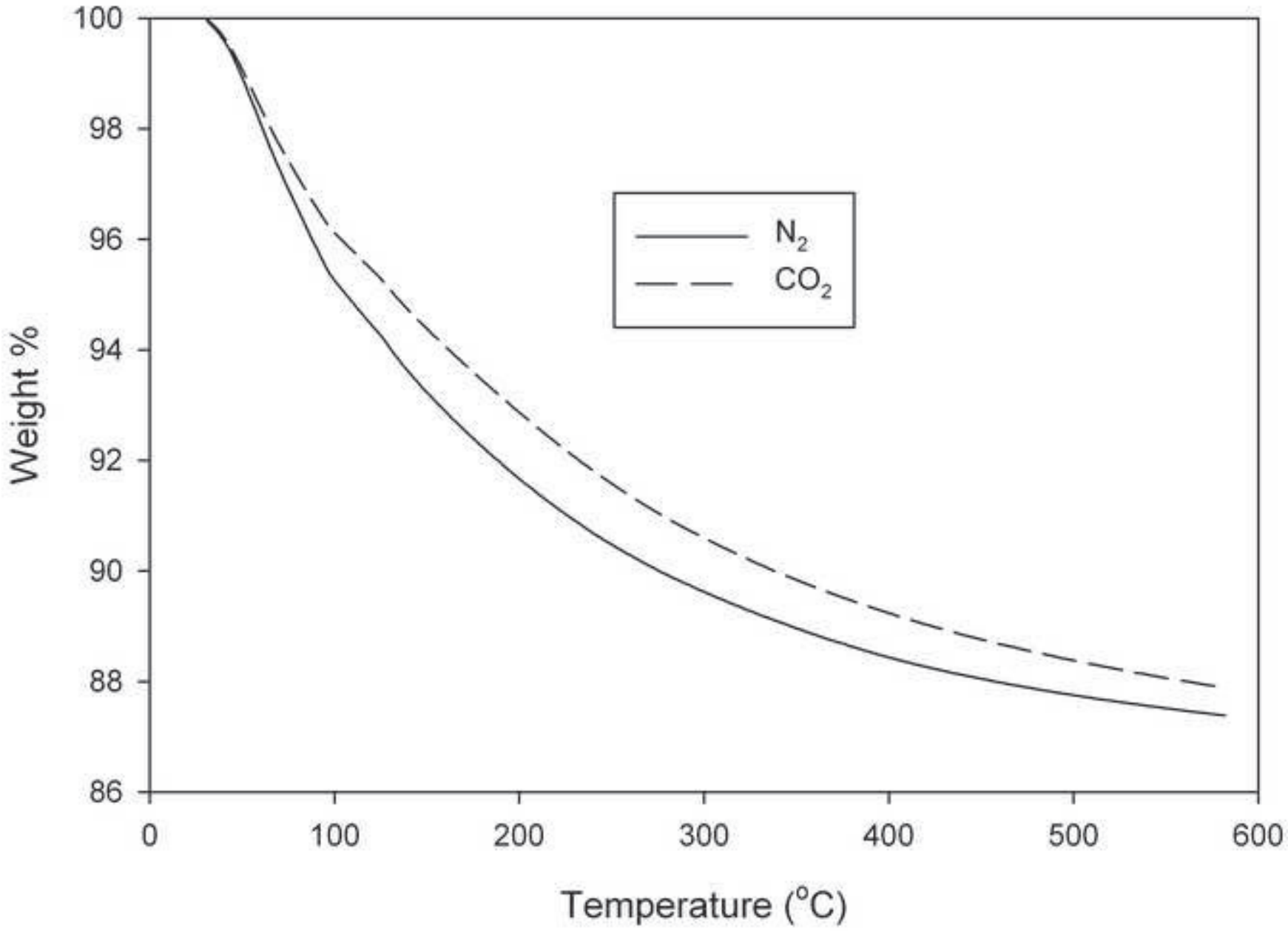

Figure 8
Click here to download high resolution image

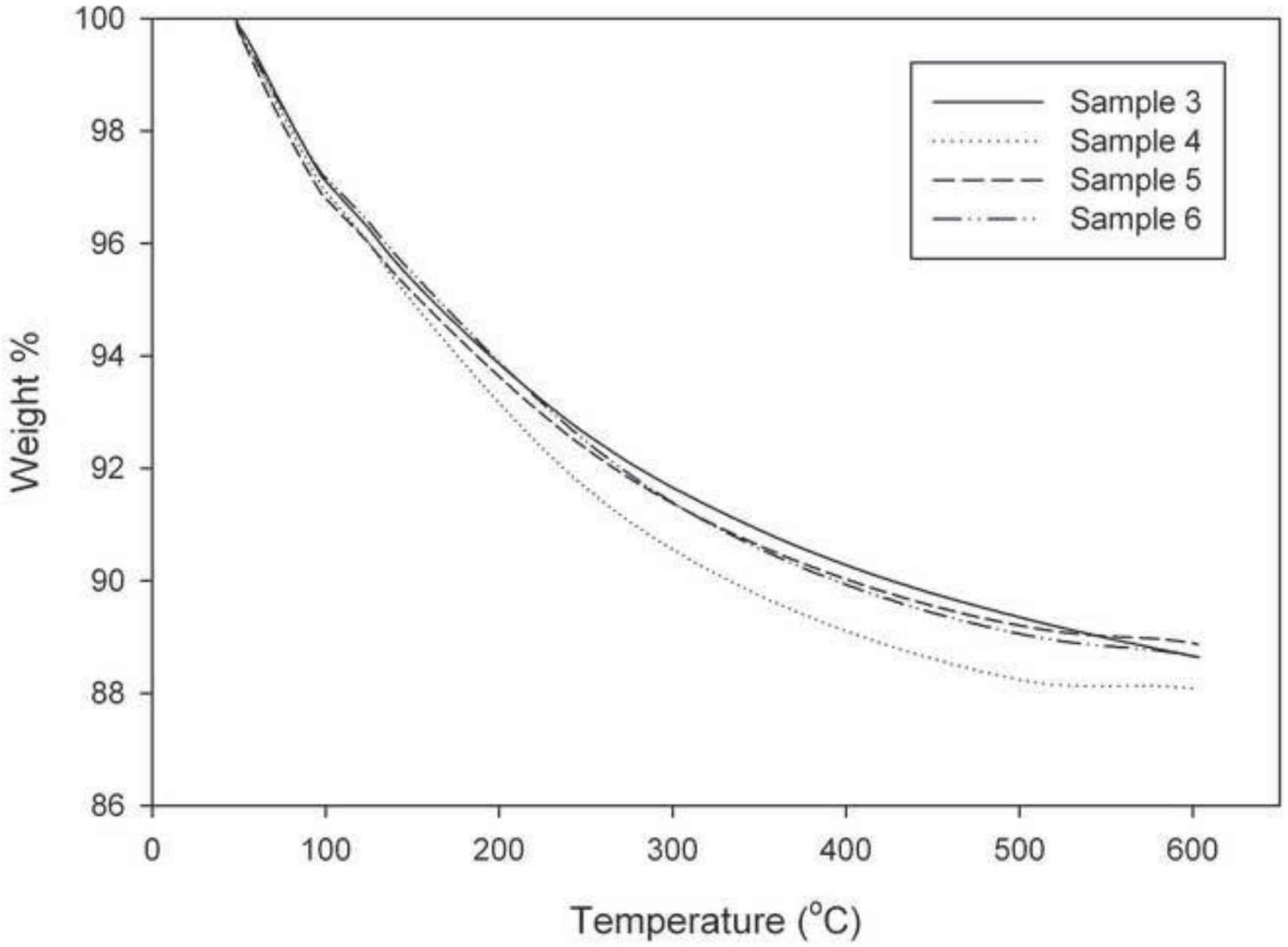

Figure 9
Click here to download high resolution image

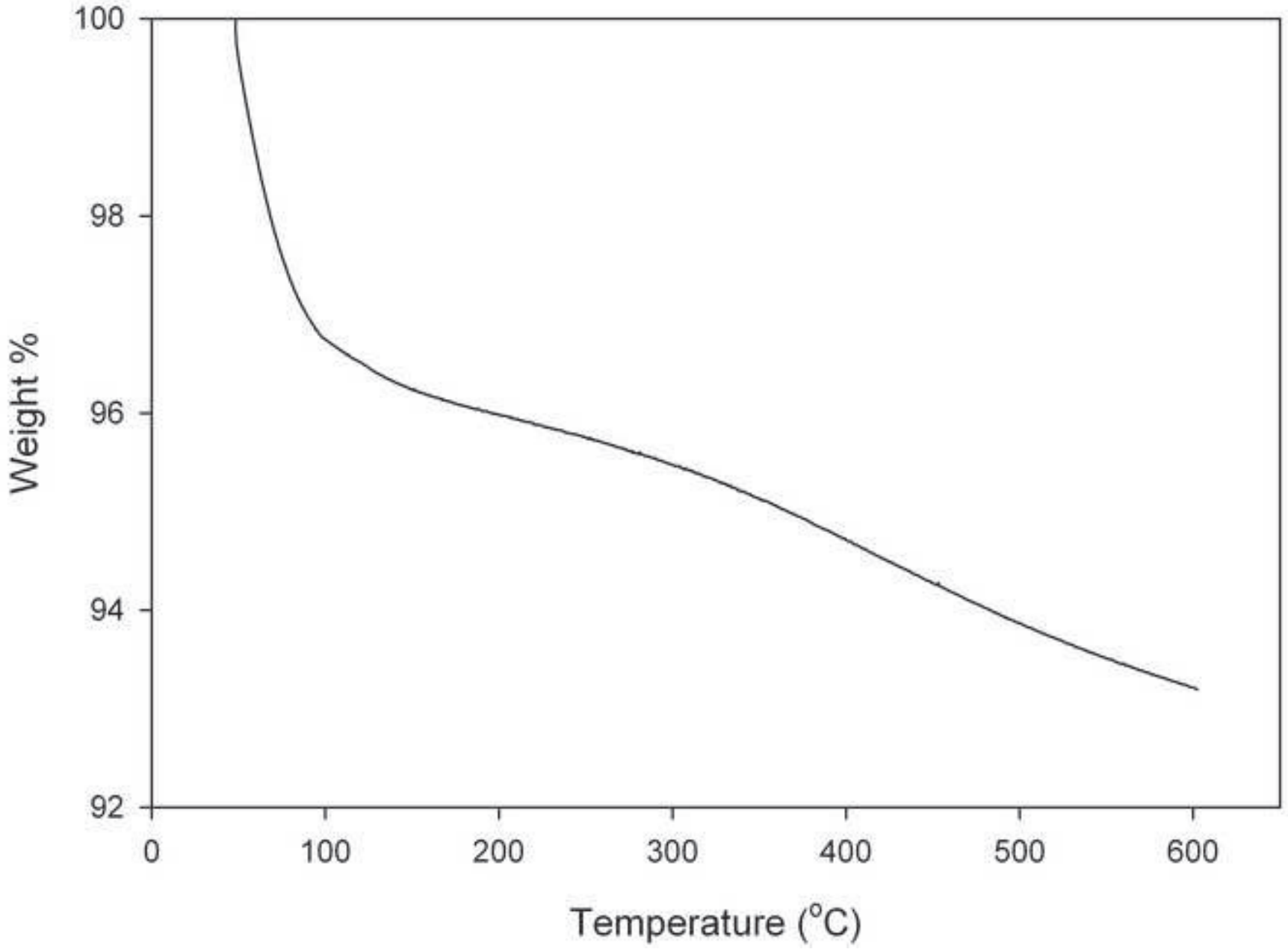

Figure 10
Click here to download high resolution image

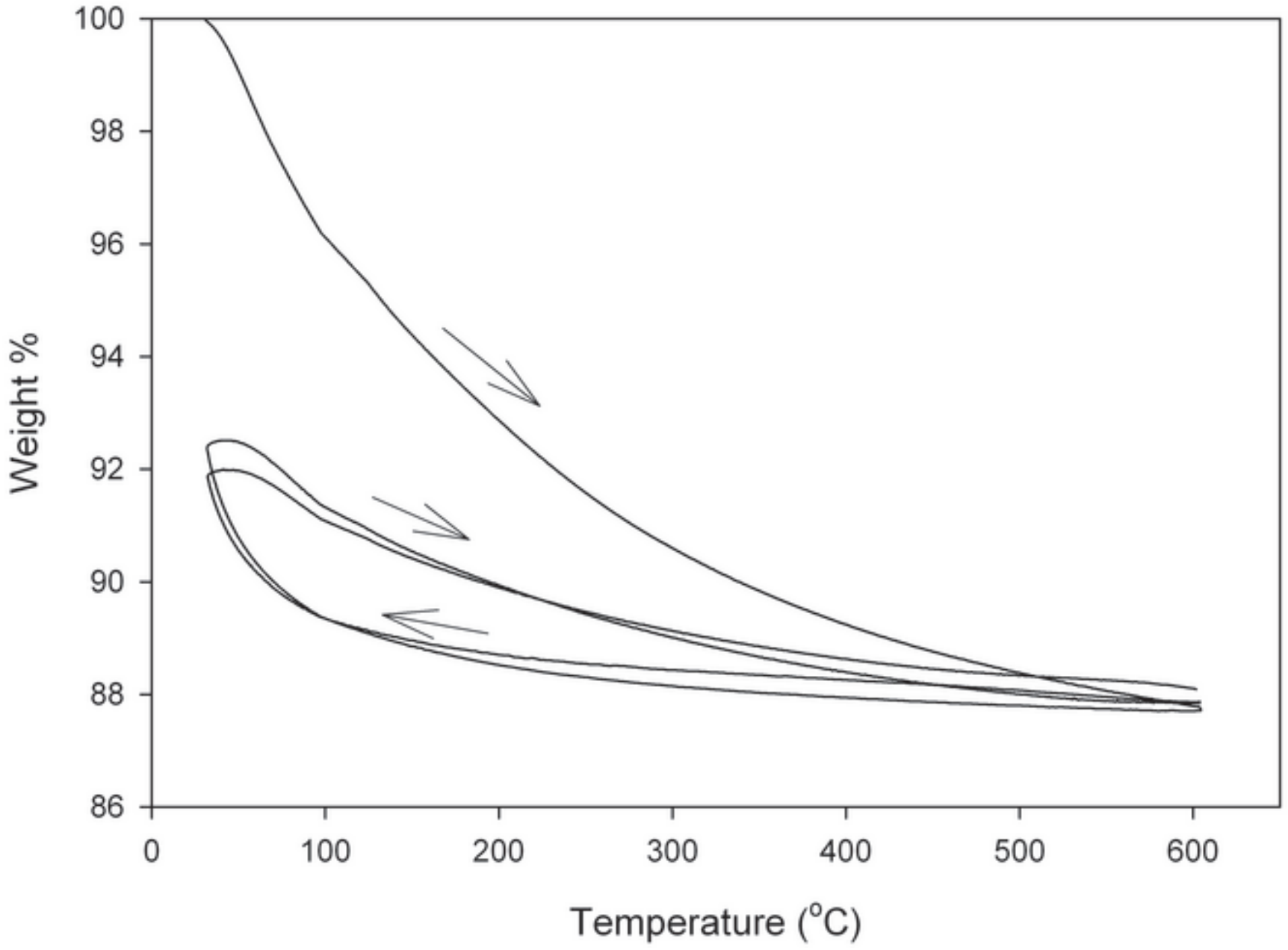

Figure 11
Click here to download high resolution image

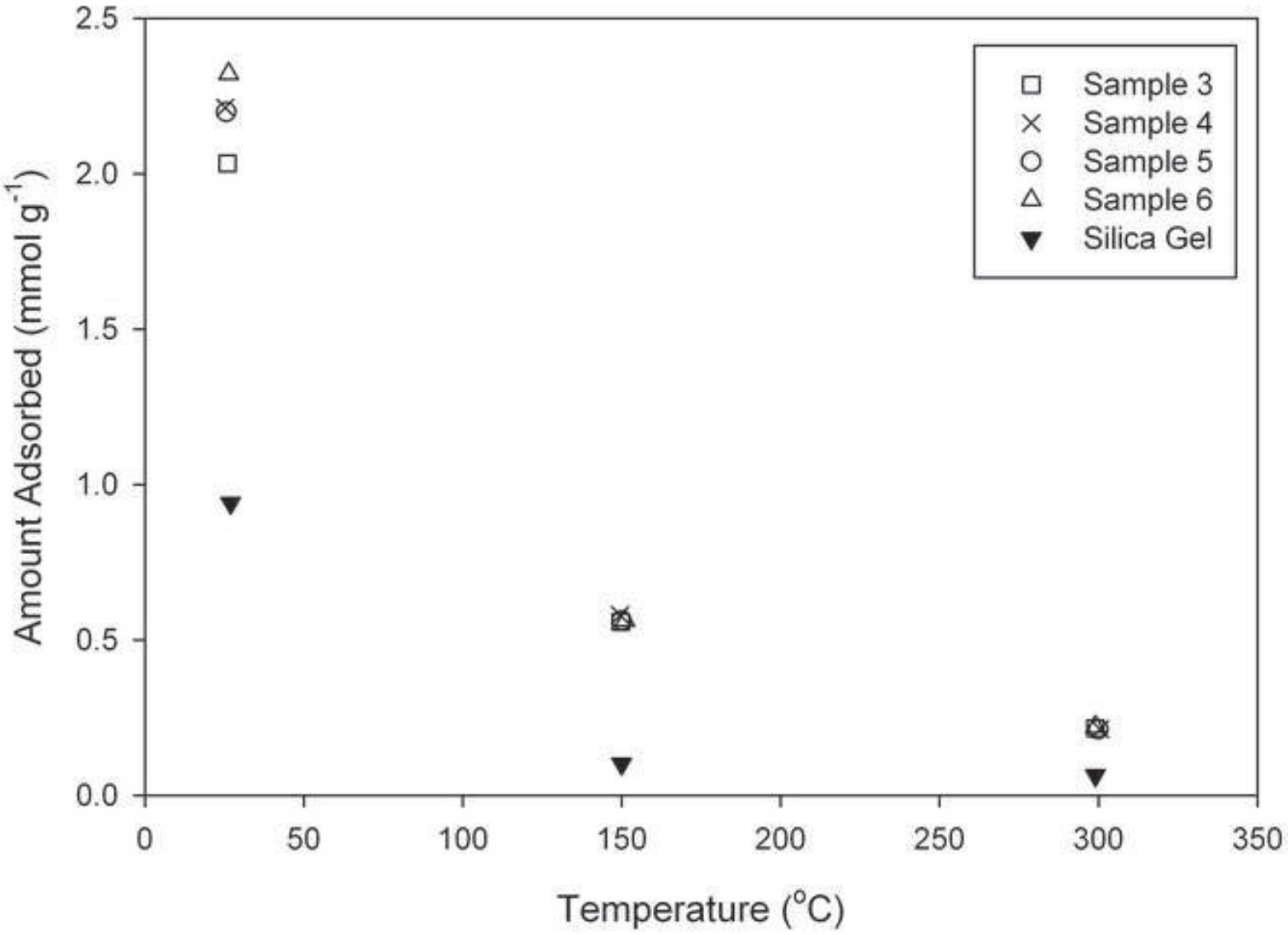

Table

Table 1. A comparison of the surface area and textural properties of various hydrotalcite derived mixed oxides. The surface areas reported for Sample 1 and 2 refer to the non-calcined form. Sample 3 – 6 were calcined at 600 °C in air.

Sample	Surface area m^2g^{-1}
Sample 1 $Ni^{2+}/Mg^{2+}/Al^{3+}$ (0.334:0.333:0.333) powder	186.7
Sample 2 $Ni^{2+}/Mg^{2+}/Al^{3+}/Fe^{3+}$ (0.334:0.333:0.233:0.1) powder	156.4
Boehmite powder	265.7± 7.8
Sample 3 $Ni^{2+}/Mg^{2+}/Al^{3+}$ (0.334:0.333:0.333) (50% Htlc:50% boehmite pellet)	234 ± 0.3
Sample 4 $Ni^{2+}/Mg^{2+}/Al^{3+}$ (0.334:0.333:0.333) (70% Htlc:30% boehmite pellet)	200 ± 0.3
Sample 5 $Ni^{2+}/Mg^{2+}/Al^{3+}/Fe^{3+}$ (0.334:0.333:0.233:0.1) (50% Htlc:50% boehmite pellet)	218 ± 0.4
Sample 6 $Ni^{2+}/Mg^{2+}/Al^{3+}/Fe^{3+}$ (0.334:0.333:0.233:0.1) (70% Htlc:30% boehmite pellet)	206 ± 1.3

Table 2. Adsorption and desorption of carbon dioxide at different pre-treatment and desorption temperatures; Sample 3 was calcined at 600 °C.

Substance	**Pre-treatment**	**CO_2 adsorption at 20 °C in mmol g^{-1}**	**Desorption temperature**	**Desorption**
Sample 3	150 °C (60 min)	1.0	150 °C	Complete
Sample 3	300 °C (60 min)	1.5	300 °C	Complete
Sample 3	600 °C (10 min)	2.0	600 °C	Complete
Sample 3	300 °C (60 min)	1.5	150 °C	1.1 mmol g^{-1} desorbed
Silica gel	150 °C (60 min)	0.9	150 °C	Complete
Silica gel	600 °C (10 min)	0.5	600 °C	Complete; some decomposition

Table 3: Adsorption of carbon dioxide on Sample 3 at 150 °C under different sample conditions.

Substance	**Form**	**Sorption cycle**	**CO_2 adsorption in mmol g^{-1}**
Sample 3	Powder	First	0.56
Sample 3	Powder	Second	0.52
Sample 3	Pellet	First	0.52